Poly-specific *trans*-acyltransferase machinery revealed via engineered acyl-CoA synthetases

Irina Koryakina[1], John McArthur[1], Shan Randall[2], Matthew Draelos[1], Ewa M Musiol[3], David C Muddiman[2], Tilmann Weber[3], & Gavin J Williams[1]*

[1] Department of Chemistry, North Carolina State University, Raleigh, NC, USA

[2] W.M. Keck FT-ICR Mass Spectrometry Laboratory, Department of Chemistry, North Carolina State University, Raleigh, NC, USA

[3] Eberhard-Karls-Universität Tűbingen, Interfakultäres Institut fűr Mikrobiologie und Infektionsmedizin, Mikrobiologie/Biotechnologie, Tűbingen, Germany

*Corresponding author, e-mail: gavin_williams@ncsu.edu

Supplementary Figures

Figure S1. Steady state kinetic analysis of WT and mutant MatB enzymes. Determination of initial velocities was performed as described in the **Supplemental Methods**. ATP and CoA were constant while **16-23**, **25-26** were varied.

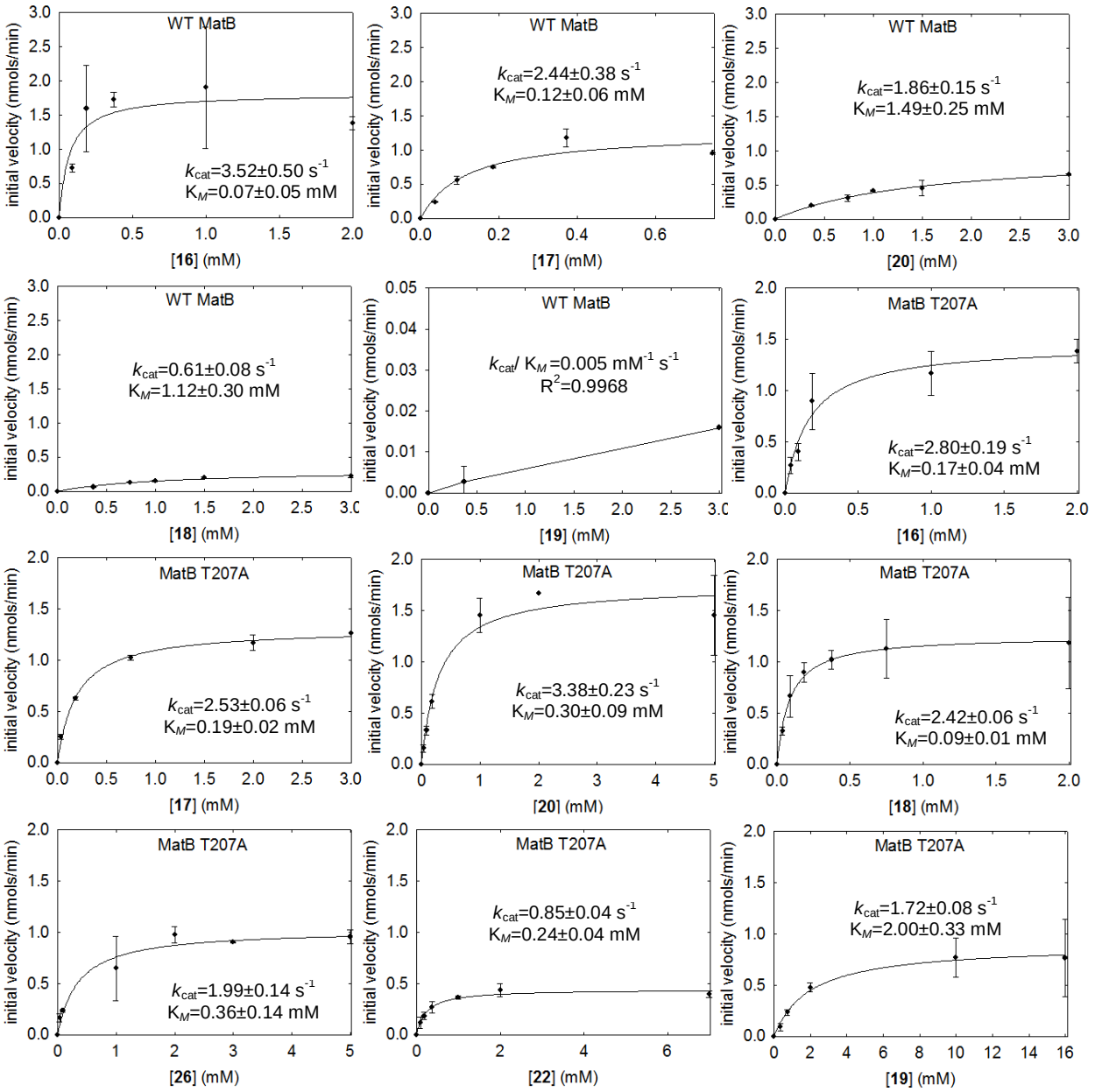

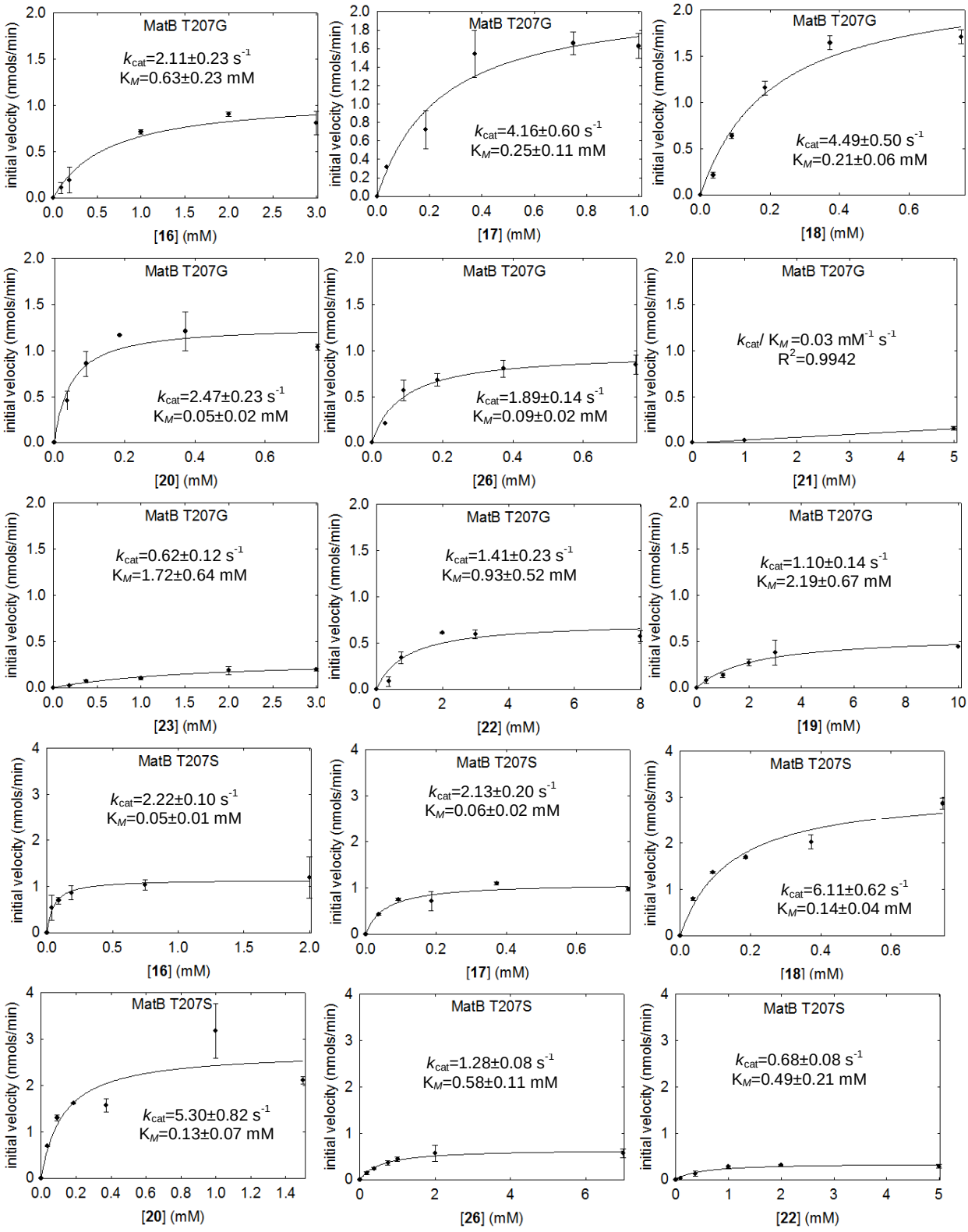
MatB T207G
k_{cat}=2.11±0.23 s^{-1}
K_M=0.63±0.23 mM
initial velocity (nmols/min)
[16] (mM)
MatB T207G
k_{cat}=4.16±0.60 s^{-1}
K_M=0.25±0.11 mM
[17] (mM)
MatB T207G
k_{cat}=4.49±0.50 s^{-1}
K_M=0.21±0.06 mM
[18] (mM)
MatB T207G
k_{cat}=2.47±0.23 s^{-1}
K_M=0.05±0.02 mM
[20] (mM)
MatB T207G
k_{cat}=1.89±0.14 s^{-1}
K_M=0.09±0.02 mM
[26] (mM)
MatB T207G
k_{cat}/ K_M=0.03 mM^{-1} s^{-1}
R^2=0.9942
[21] (mM)
MatB T207G
k_{cat}=0.62±0.12 s^{-1}
K_M=1.72±0.64 mM
[23] (mM)
MatB T207G
k_{cat}=1.41±0.23 s^{-1}
K_M=0.93±0.52 mM
[22] (mM)
MatB T207G
k_{cat}=1.10±0.14 s^{-1}
K_M=2.19±0.67 mM
[19] (mM)
MatB T207S
k_{cat}=2.22±0.10 s^{-1}
K_M=0.05±0.01 mM
[16] (mM)
MatB T207S
k_{cat}=2.13±0.20 s^{-1}
K_M=0.06±0.02 mM
[17] (mM)
MatB T207S
k_{cat}=6.11±0.62 s^{-1}
K_M=0.14±0.04 mM
[18] (mM)
MatB T207S
k_{cat}=5.30±0.82 s^{-1}
K_M=0.13±0.07 mM
[20] (mM)
MatB T207S
k_{cat}=1.28±0.08 s^{-1}
K_M=0.58±0.11 mM
[26] (mM)
MatB T207S
k_{cat}=0.68±0.08 s^{-1}
K_M=0.49±0.21 mM
[22] (mM)

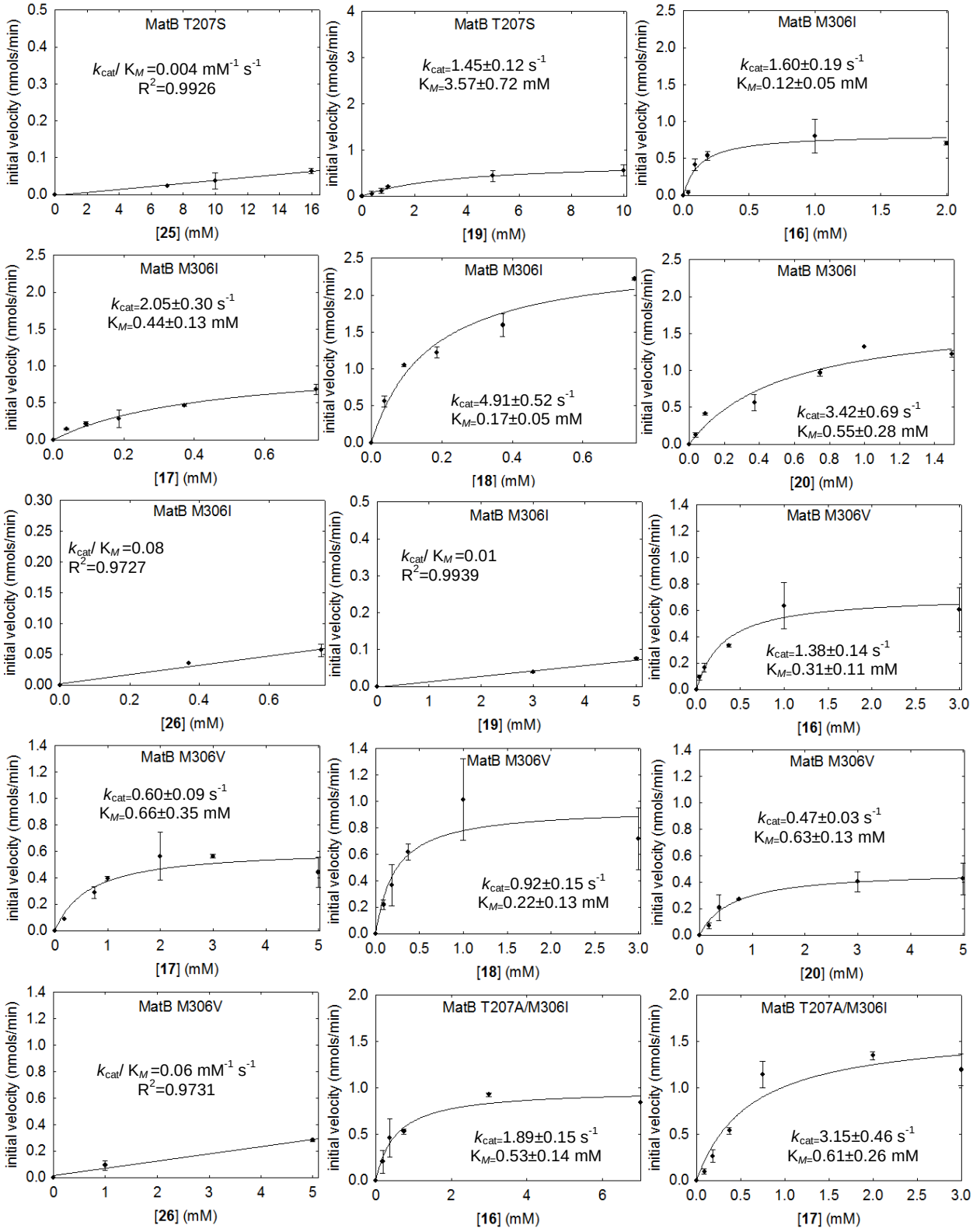
MatB T207S
k_{cat}/ K_M =0.004 mM^{-1} s^{-1}
R^2=0.9926
initial velocity (nmols/min)
[25] (mM)
MatB T207S
k_{cat}=1.45±0.12 s^{-1}
K_M=3.57±0.72 mM
initial velocity (nmols/min)
[19] (mM)
MatB M306I
k_{cat}=1.60±0.19 s^{-1}
K_M=0.12±0.05 mM
initial velocity (nmols/min)
[16] (mM)
MatB M306I
k_{cat}=2.05±0.30 s^{-1}
K_M=0.44±0.13 mM
initial velocity (nmols/min)
[17] (mM)
MatB M306I
k_{cat}=4.91±0.52 s^{-1}
K_M=0.17±0.05 mM
initial velocity (nmols/min)
[18] (mM)
MatB M306I
k_{cat}=3.42±0.69 s^{-1}
K_M=0.55±0.28 mM
initial velocity (nmols/min)
[20] (mM)
MatB M306I
k_{cat}/ K_M =0.08
R^2=0.9727
initial velocity (nmols/min)
[26] (mM)
MatB M306I
k_{cat}/ K_M =0.01
R^2=0.9939
initial velocity (nmols/min)
[19] (mM)
MatB M306V
k_{cat}=1.38±0.14 s^{-1}
K_M=0.31±0.11 mM
initial velocity (nmols/min)
[16] (mM)
MatB M306V
k_{cat}=0.60±0.09 s^{-1}
K_M=0.66±0.35 mM
initial velocity (nmols/min)
[17] (mM)
MatB M306V
k_{cat}=0.92±0.15 s^{-1}
K_M=0.22±0.13 mM
initial velocity (nmols/min)
[18] (mM)
MatB M306V
k_{cat}=0.47±0.03 s^{-1}
K_M=0.63±0.13 mM
initial velocity (nmols/min)
[20] (mM)
MatB M306V
k_{cat}/ K_M =0.06 mM^{-1} s^{-1}
R^2=0.9731
initial velocity (nmols/min)
[26] (mM)
MatB T207A/M306I
k_{cat}=1.89±0.15 s^{-1}
K_M=0.53±0.14 mM
initial velocity (nmols/min)
[16] (mM)
MatB T207A/M306I
k_{cat}=3.15±0.46 s^{-1}
K_M=0.61±0.26 mM
initial velocity (nmols/min)
[17] (mM)

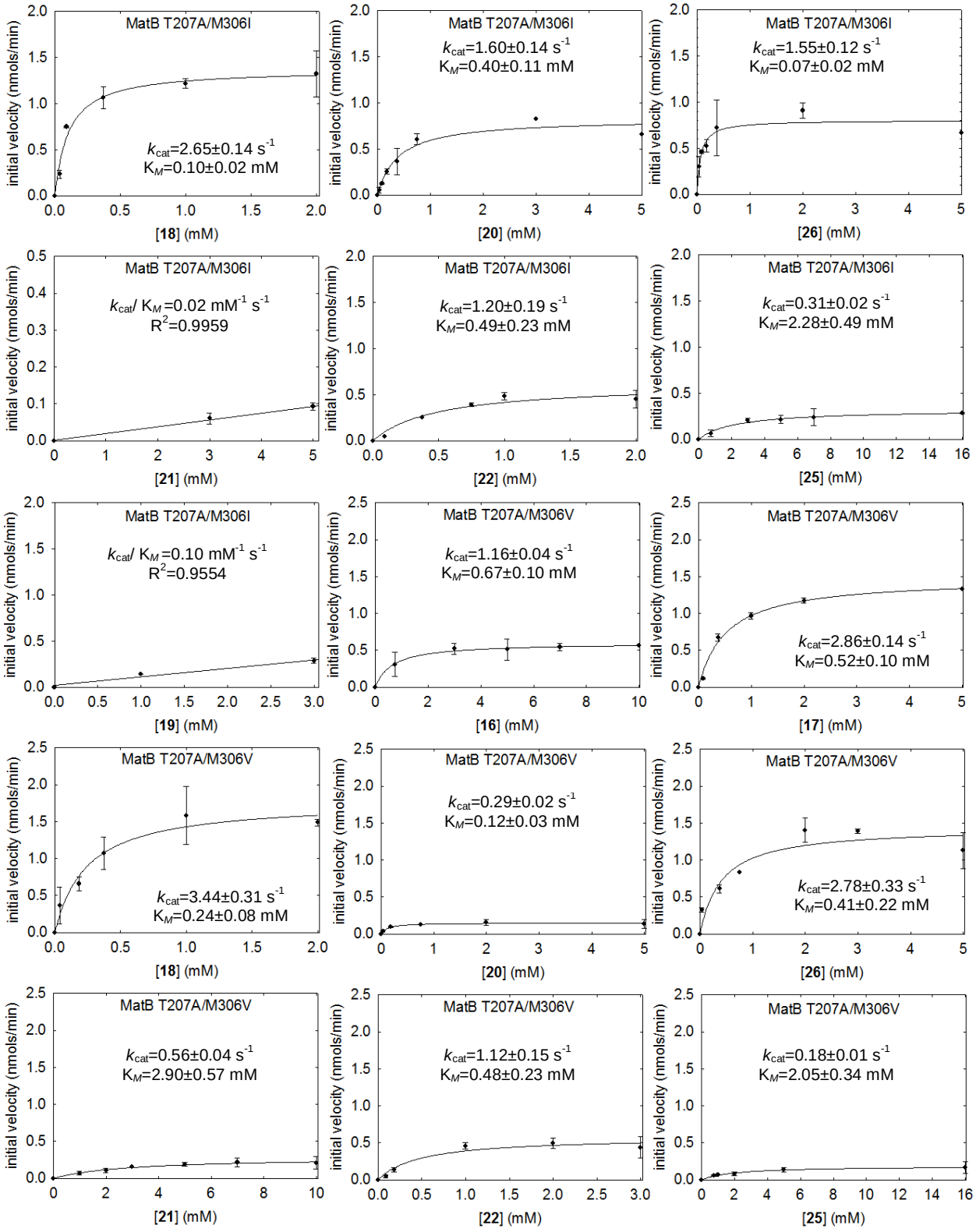
MatB T207A/M306I
k_{cat}=2.65±0.14 s^{-1}
K_M=0.10±0.02 mM
initial velocity (nmols/min)
[18] (mM)
MatB T207A/M306I
k_{cat}=1.60±0.14 s^{-1}
K_M=0.40±0.11 mM
[20] (mM)
MatB T207A/M306I
k_{cat}=1.55±0.12 s^{-1}
K_M=0.07±0.02 mM
[26] (mM)
MatB T207A/M306I
k_{cat}/ K_M=0.02 mM^{-1} s^{-1}
R^2=0.9959
[21] (mM)
MatB T207A/M306I
k_{cat}=1.20±0.19 s^{-1}
K_M=0.49±0.23 mM
[22] (mM)
MatB T207A/M306I
k_{cat}=0.31±0.02 s^{-1}
K_M=2.28±0.49 mM
[25] (mM)
MatB T207A/M306I
k_{cat}/ K_M=0.10 mM^{-1} s^{-1}
R^2=0.9554
[19] (mM)
MatB T207A/M306V
k_{cat}=1.16±0.04 s^{-1}
K_M=0.67±0.10 mM
[16] (mM)
MatB T207A/M306V
k_{cat}=2.86±0.14 s^{-1}
K_M=0.52±0.10 mM
[17] (mM)
MatB T207A/M306V
k_{cat}=3.44±0.31 s^{-1}
K_M=0.24±0.08 mM
[18] (mM)
MatB T207A/M306V
k_{cat}=0.29±0.02 s^{-1}
K_M=0.12±0.03 mM
[20] (mM)
MatB T207A/M306V
k_{cat}=2.78±0.33 s^{-1}
K_M=0.41±0.22 mM
[26] (mM)
MatB T207A/M306V
k_{cat}=0.56±0.04 s^{-1}
K_M=2.90±0.57 mM
[21] (mM)
MatB T207A/M306V
k_{cat}=1.12±0.15 s^{-1}
K_M=0.48±0.23 mM
[22] (mM)
MatB T207A/M306V
k_{cat}=0.18±0.01 s^{-1}
K_M=2.05±0.34 mM
[25] (mM)

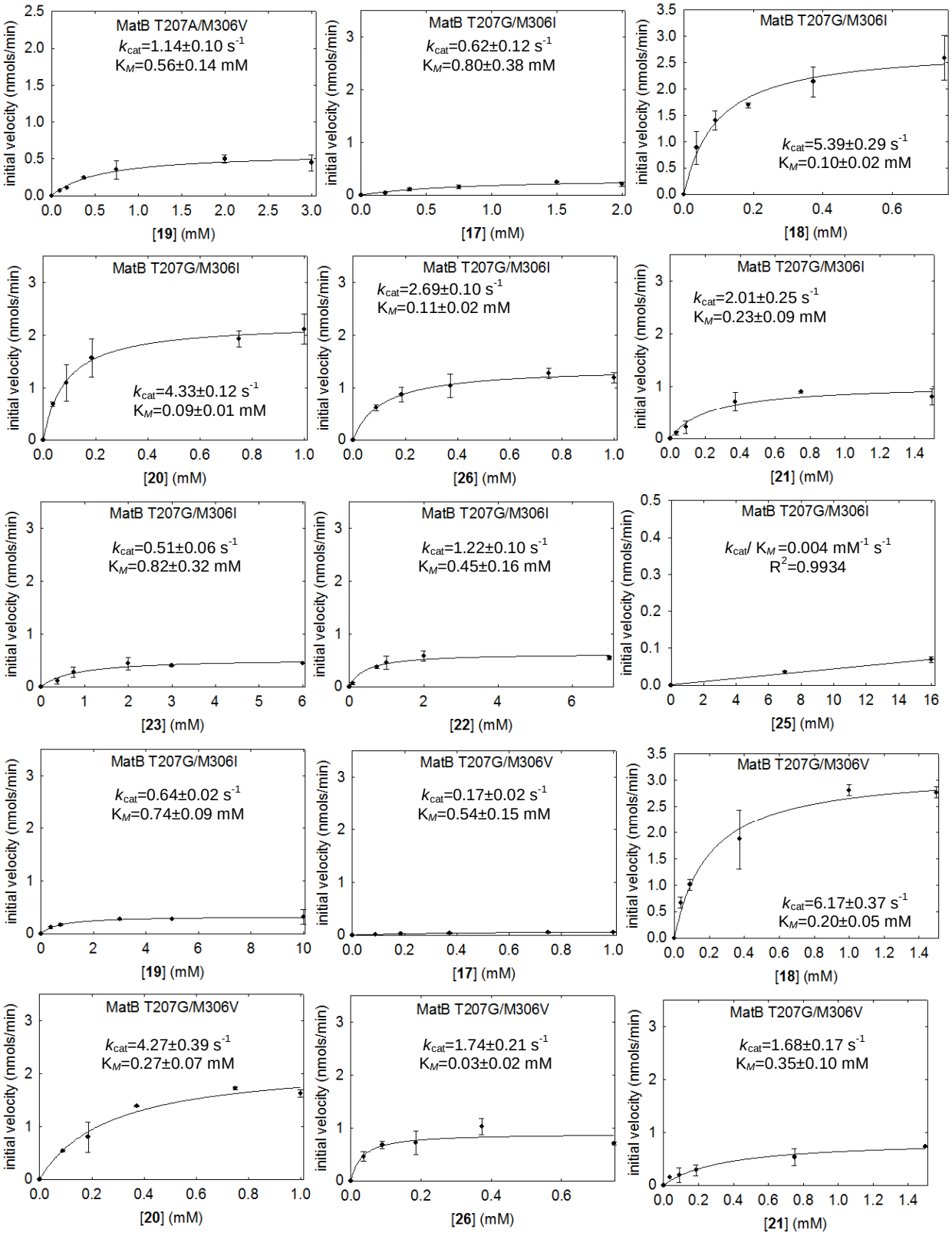
MatB T207A/M306V
k_{cat}=1.14±0.10 s^{-1}
K_M=0.56±0.14 mM
initial velocity (nmols/min)
[19] (mM)
MatB T207G/M306I
k_{cat}=0.62±0.12 s^{-1}
K_M=0.80±0.38 mM
initial velocity (nmols/min)
[17] (mM)
MatB T207G/M306I
k_{cat}=5.39±0.29 s^{-1}
K_M=0.10±0.02 mM
initial velocity (nmols/min)
[18] (mM)
MatB T207G/M306I
k_{cat}=4.33±0.12 s^{-1}
K_M=0.09±0.01 mM
initial velocity (nmols/min)
[20] (mM)
MatB T207G/M306I
k_{cat}=2.69±0.10 s^{-1}
K_M=0.11±0.02 mM
initial velocity (nmols/min)
[26] (mM)
MatB T207G/M306I
k_{cat}=2.01±0.25 s^{-1}
K_M=0.23±0.09 mM
initial velocity (nmols/min)
[21] (mM)
MatB T207G/M306I
k_{cat}=0.51±0.06 s^{-1}
K_M=0.82±0.32 mM
initial velocity (nmols/min)
[23] (mM)
MatB T207G/M306I
k_{cat}=1.22±0.10 s^{-1}
K_M=0.45±0.16 mM
initial velocity (nmols/min)
[22] (mM)
MatB T207G/M306I
k_{cat}/ K_M =0.004 mM^{-1} s^{-1}
R^2=0.9934
initial velocity (nmols/min)
[25] (mM)
MatB T207G/M306I
k_{cat}=0.64±0.02 s^{-1}
K_M=0.74±0.09 mM
initial velocity (nmols/min)
[19] (mM)
MatB T207G/M306V
k_{cat}=0.17±0.02 s^{-1}
K_M=0.54±0.15 mM
initial velocity (nmols/min)
[17] (mM)
MatB T207G/M306V
k_{cat}=6.17±0.37 s^{-1}
K_M=0.20±0.05 mM
initial velocity (nmols/min)
[18] (mM)
MatB T207G/M306V
k_{cat}=4.27±0.39 s^{-1}
K_M=0.27±0.07 mM
initial velocity (nmols/min)
[20] (mM)
MatB T207G/M306V
k_{cat}=1.74±0.21 s^{-1}
K_M=0.03±0.02 mM
initial velocity (nmols/min)
[26] (mM)
MatB T207G/M306V
k_{cat}=1.68±0.17 s^{-1}
K_M=0.35±0.10 mM
initial velocity (nmols/min)
[21] (mM)

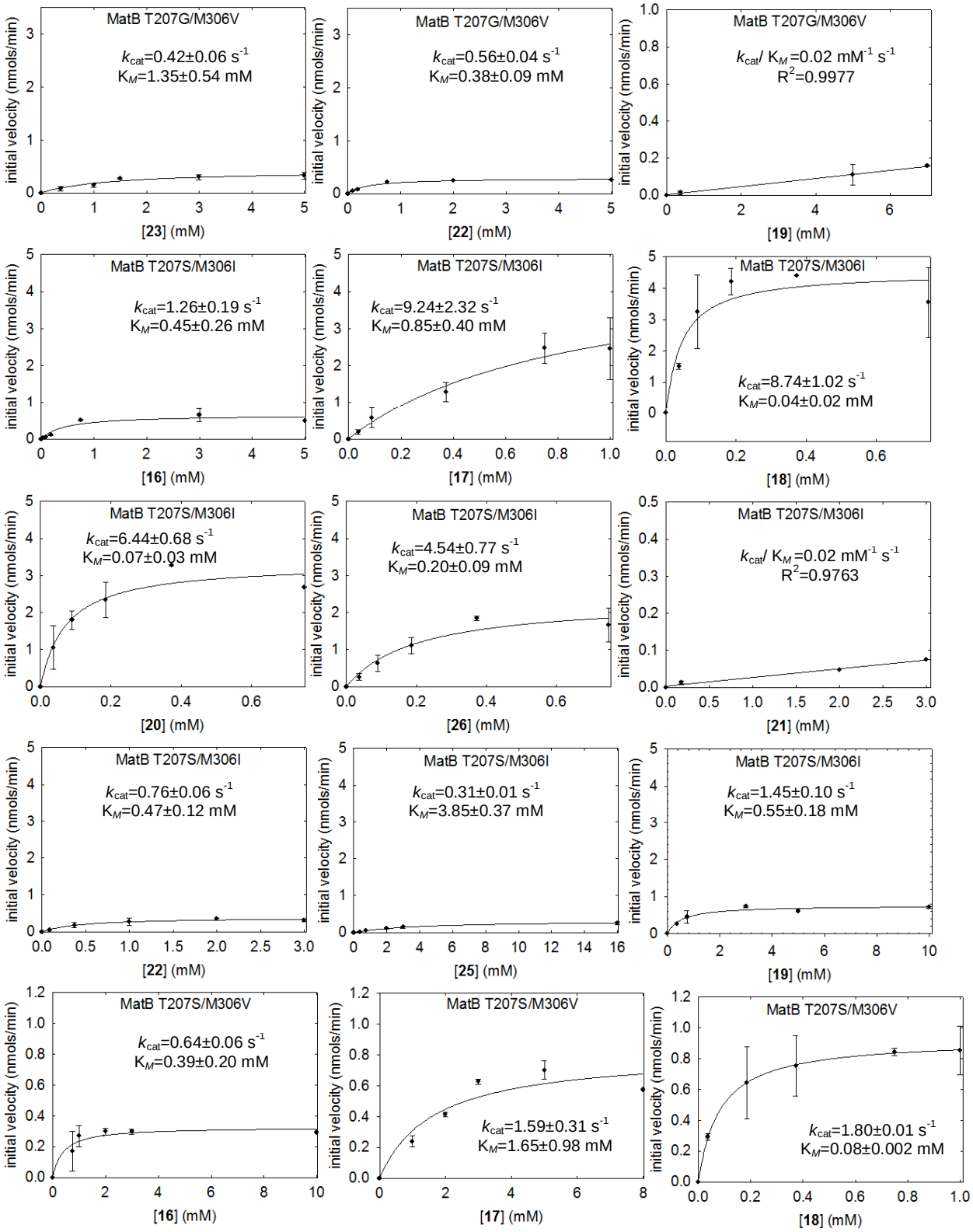
MatB T207G/M306V
k_{cat}=0.42±0.06 s^{-1}
K_M=1.35±0.54 mM
initial velocity (nmols/min)
[23] (mM)
MatB T207G/M306V
k_{cat}=0.56±0.04 s^{-1}
K_M=0.38±0.09 mM
initial velocity (nmols/min)
[22] (mM)
MatB T207G/M306V
k_{cat}/ K_M=0.02 mM^{-1} s^{-1}
R^2=0.9977
initial velocity (nmols/min)
[19] (mM)
MatB T207S/M306I
k_{cat}=1.26±0.19 s^{-1}
K_M=0.45±0.26 mM
initial velocity (nmols/min)
[16] (mM)
MatB T207S/M306I
k_{cat}=9.24±2.32 s^{-1}
K_M=0.85±0.40 mM
initial velocity (nmols/min)
[17] (mM)
MatB T207S/M306I
k_{cat}=8.74±1.02 s^{-1}
K_M=0.04±0.02 mM
initial velocity (nmols/min)
[18] (mM)
MatB T207S/M306I
k_{cat}=6.44±0.68 s^{-1}
K_M=0.07±0.03 mM
initial velocity (nmols/min)
[20] (mM)
MatB T207S/M306I
k_{cat}=4.54±0.77 s^{-1}
K_M=0.20±0.09 mM
initial velocity (nmols/min)
[26] (mM)
MatB T207S/M306I
k_{cat}/ K_M=0.02 mM^{-1} s^{-1}
R^2=0.9763
initial velocity (nmols/min)
[21] (mM)
MatB T207S/M306I
k_{cat}=0.76±0.06 s^{-1}
K_M=0.47±0.12 mM
initial velocity (nmols/min)
[22] (mM)
MatB T207S/M306I
k_{cat}=0.31±0.01 s^{-1}
K_M=3.85±0.37 mM
initial velocity (nmols/min)
[25] (mM)
MatB T207S/M306I
k_{cat}=1.45±0.10 s^{-1}
K_M=0.55±0.18 mM
initial velocity (nmols/min)
[19] (mM)
MatB T207S/M306V
k_{cat}=0.64±0.06 s^{-1}
K_M=0.39±0.20 mM
initial velocity (nmols/min)
[16] (mM)
MatB T207S/M306V
k_{cat}=1.59±0.31 s^{-1}
K_M=1.65±0.98 mM
initial velocity (nmols/min)
[17] (mM)
MatB T207S/M306V
k_{cat}=1.80±0.01 s^{-1}
K_M=0.08±0.002 mM
initial velocity (nmols/min)
[18] (mM)

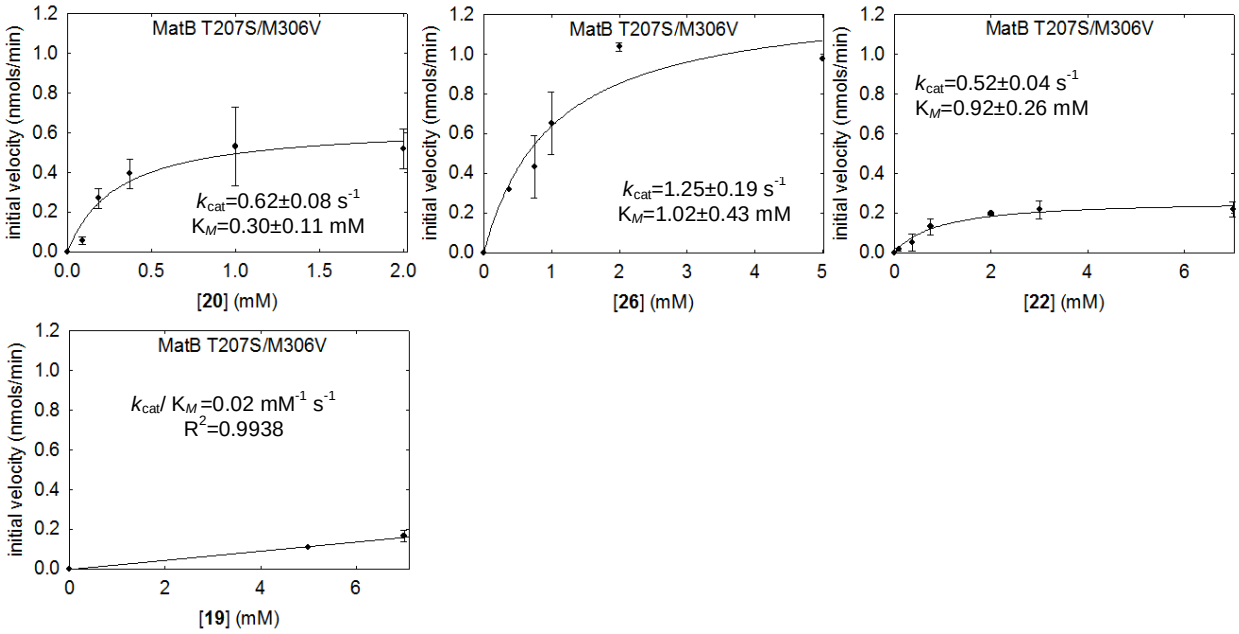
MatB T207S/M306V
initial velocity (nmols/min)
k_{cat}=0.62±0.08 s^{-1}
K_M=0.30±0.11 mM
[**20**] (mM)
MatB T207S/M306V
initial velocity (nmols/min)
k_{cat}=1.25±0.19 s^{-1}
K_M=1.02±0.43 mM
[**26**] (mM)
MatB T207S/M306V
initial velocity (nmols/min)
k_{cat}=0.52±0.04 s^{-1}
K_M=0.92±0.26 mM
[**22**] (mM)
MatB T207S/M306V
initial velocity (nmols/min)
k_{cat}/K_M=0.02 mM^{-1} s^{-1}
R^2=0.9938
[**19**] (mM)

Figure S2. RP-HPLC analysis of wild-type and variant MatB T207G/M306I catalyzed reactions using the malonate analogues (i) **16**, (ii) **17**, (iii) **18**, (iv) **19**, (v) **20**, (vi) **21**, (vii) **22**, (viii) **23**, (ix) **24**, (x) **25**, (xi) **26**. See **Experimental Section** for assay conditions and detection methods.

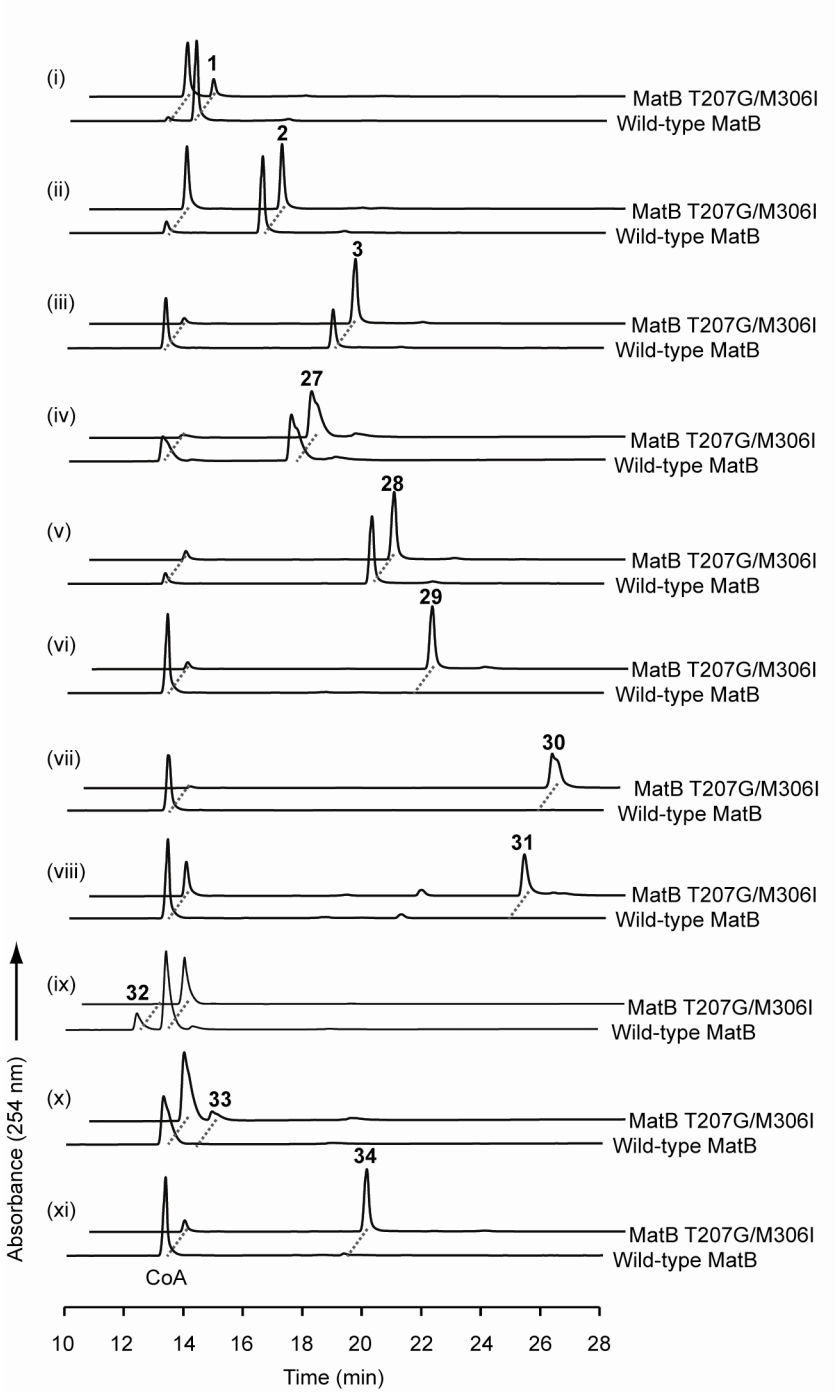

Figure S3. LC/MS-analysis of in vivo *apo*-ACP to *holo*-ACP conversion.

A) DEBS *holo*-ACP6

Deconvoluted spectra:

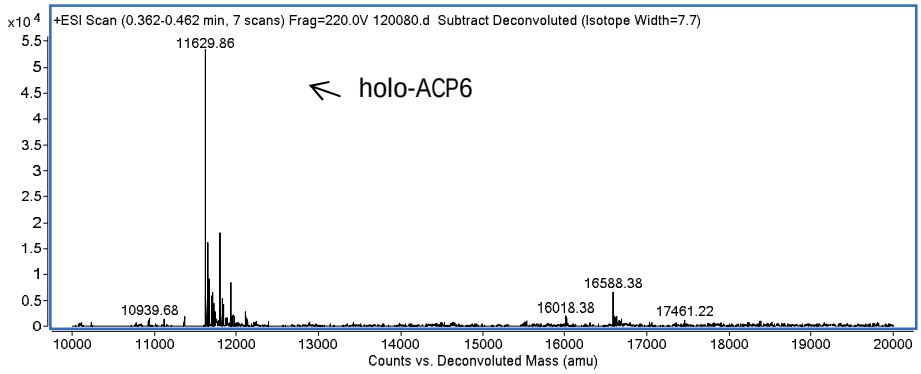

Deconvoluted spectra expanded on target peak (*holo*-ACP6):

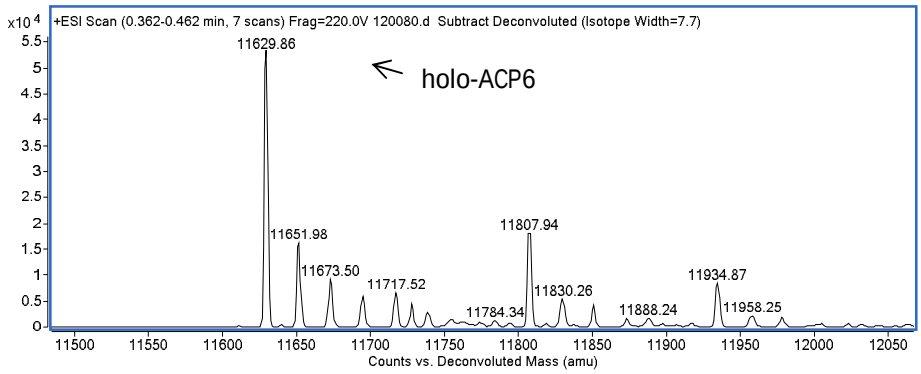

Deconvoluted spectra expanded on target peak (*apo*-ACP6)

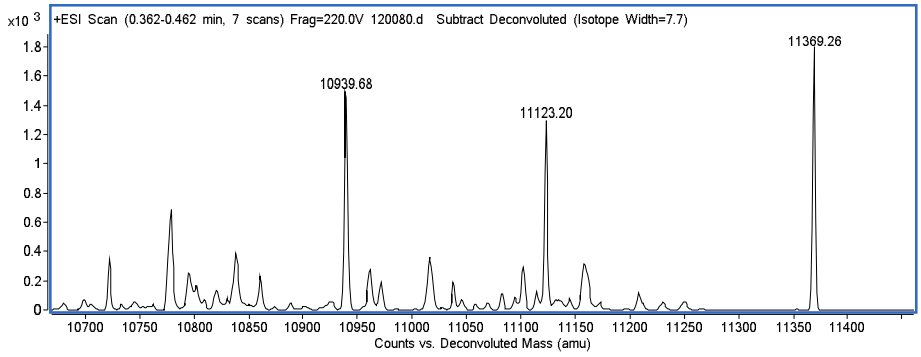

Component m/z:

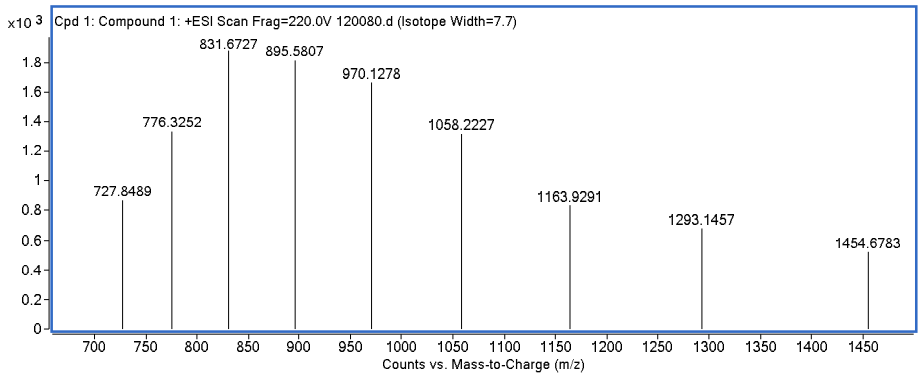

Component charge state:

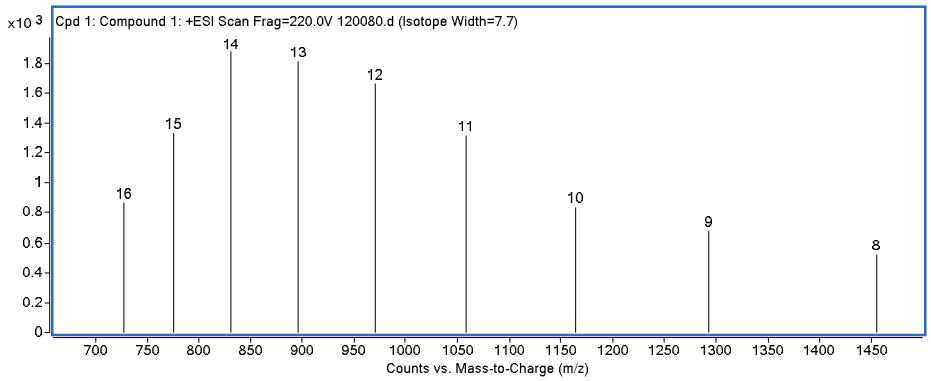

B) Kir *holo*-ACP5

Deconvoluted spectra:

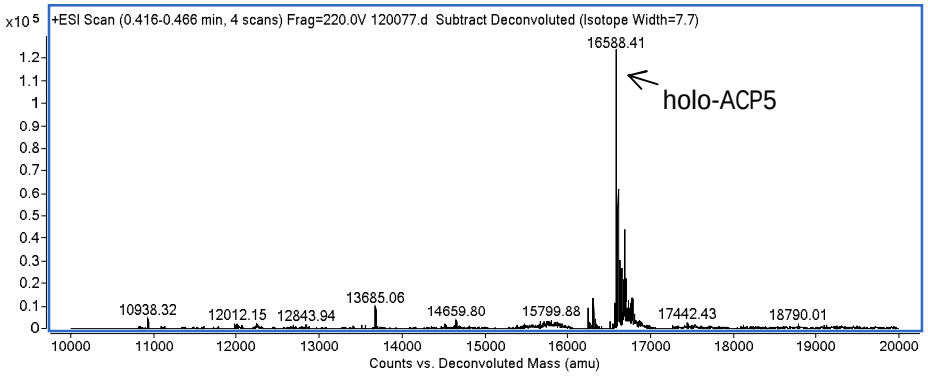

Deconvoluted spectra expanded on target peak (*holo*-ACP5):

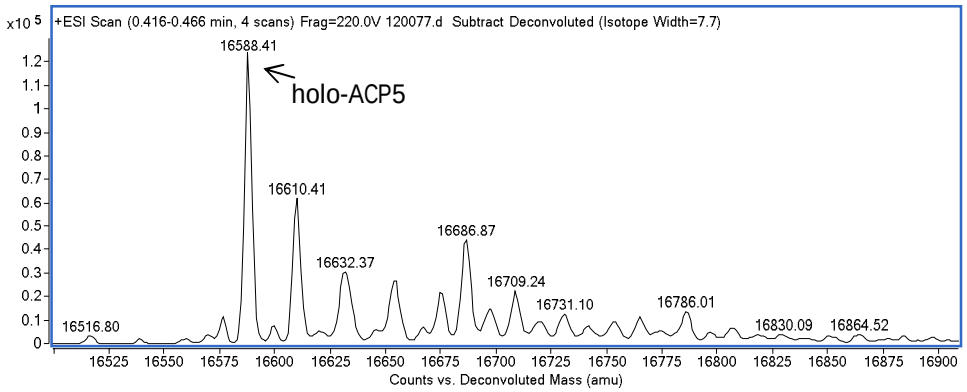

Deconvoluted spectra expanded on target peak (*apo*-ACP5):

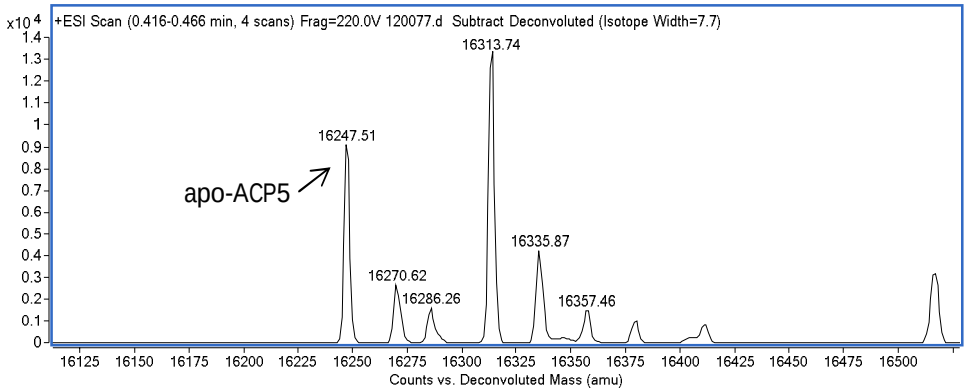

Component m/z:

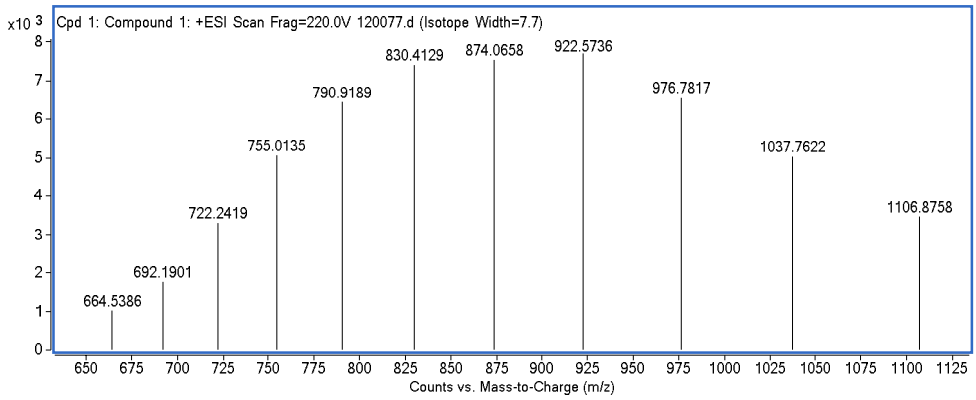

Component charge state:

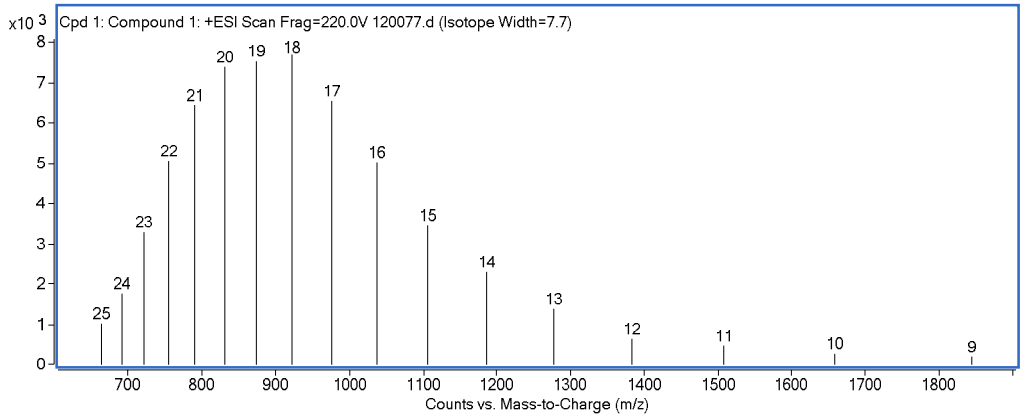

Figure S4. [1]H-NMR (300 MHz, D_2O) of methoxymalonate (**25**). See **Supporting Methods** for detailed synthesis.

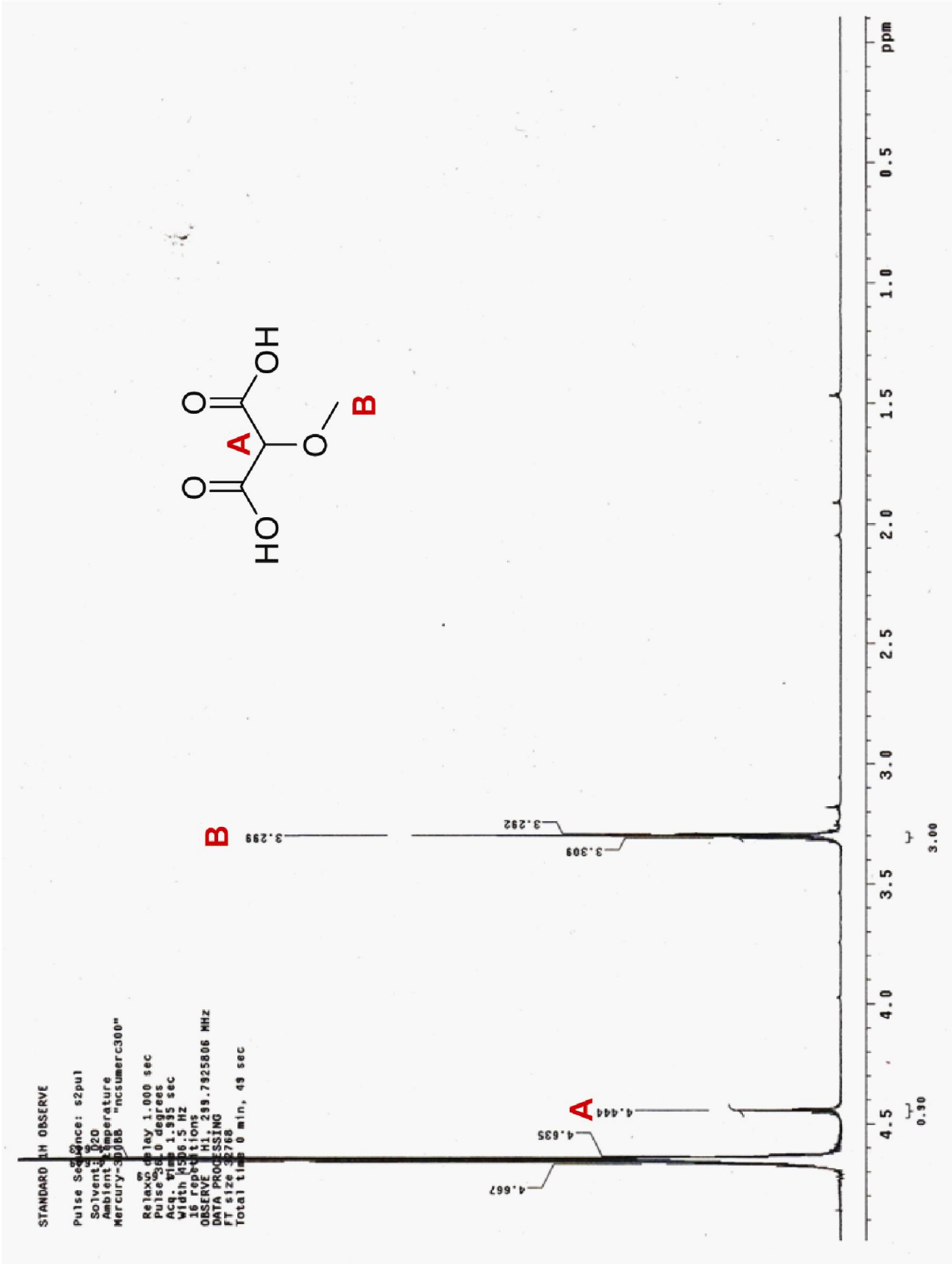

Figure S5. ^{1}H-NMR (300 MHz, D_2O) of azidoethylmalonate (**26**). See **Supporting Methods** for detailed synthesis.

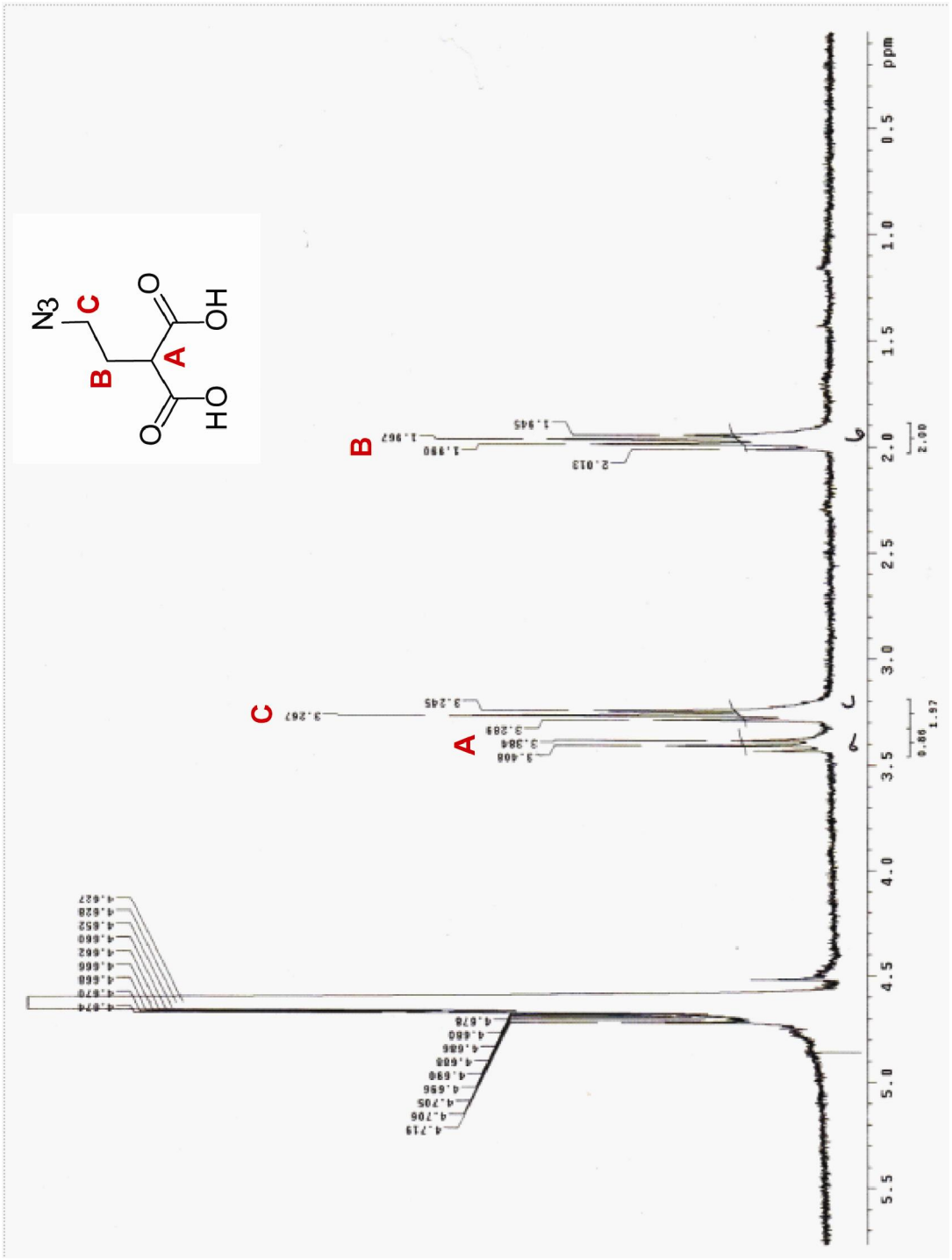

Figure S6. ^{1}H-NMR (300 MHz, D_2O) of propargylmalonate (**19**). See **Supporting Methods** for detailed synthesis.

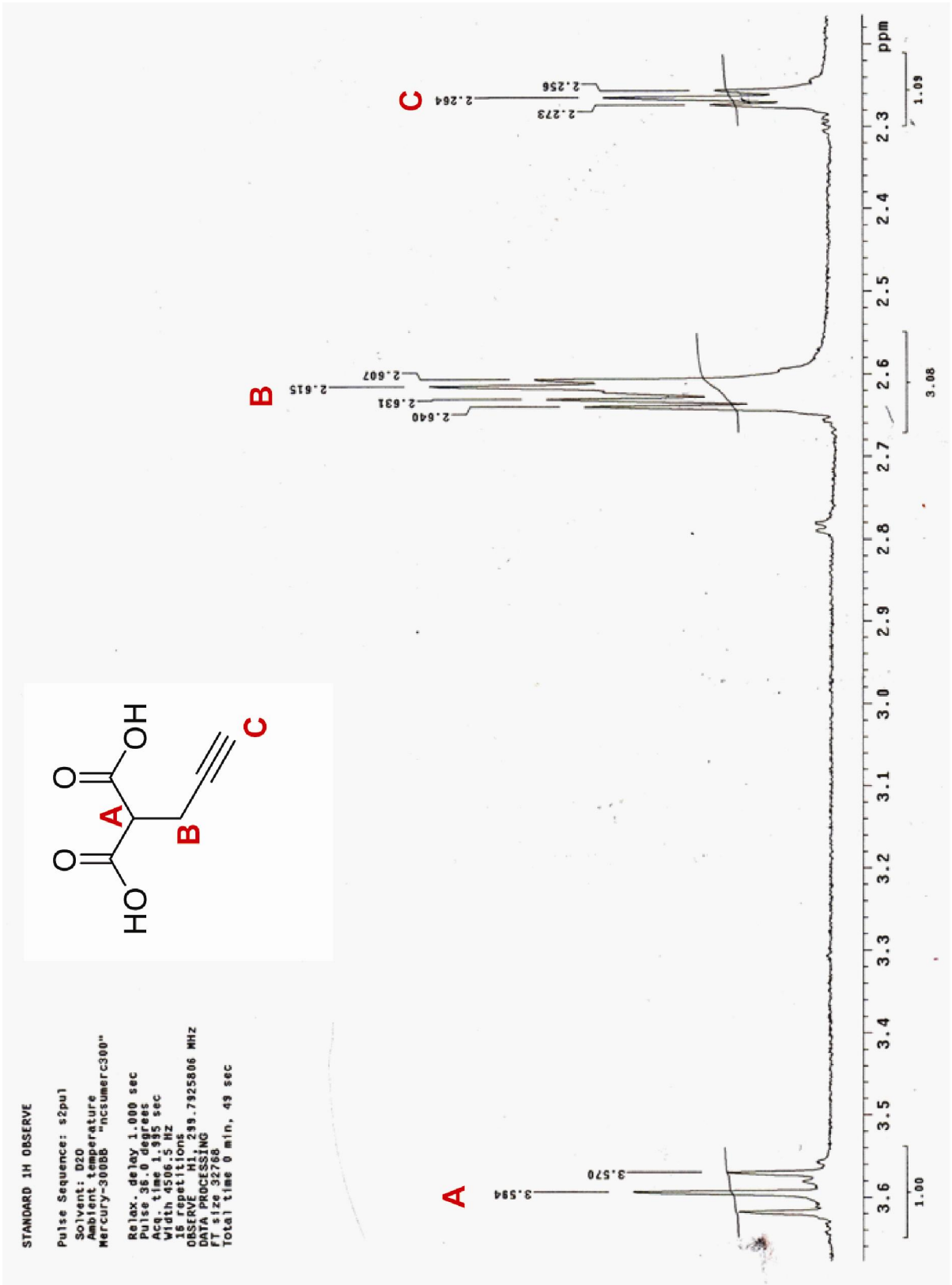

Figure S7. Protein sequences used for exact mass determinations.

Kir ACP5 (substrate for KirCII experiments):

MASWSHPQFEKGALEVLFQGPGPEPAAAVPAPPAESAPAPAATAAGGDPESAVRDHVRTLLAA
HLGMAPDRLPPDRVLSDVGVDSLGLRRLSRRLGATYGVDIPARMFGVGQTVRALARAVHDKYG
PLPATATPEPNALVPRGSSAHHHHHHHHHH

DEBS ACP6 (MCAT and DSZS experiments):

MGSSHHHHHHSSGLVPRGSHMAAPAREMTSQELLEFTHSHVAAILGHSSPDAVGQDQPFTELGF
DSLTAVGLRNQLQQATGLALPATLVFEHPTVRRLADHIGQQL

Supplementary Tables

Table S1. Steady state kinetic analysis of wild-type and MatB mutants.

Enzyme	Parameter	Malonate analog									
		16	**17**	**18**	**19**	**20**	**21**	**22**	**23**	**25**	**26**
WT	k_{cat} (s^{-1})	3.52 ±0.50	2.44 ±0.38	0.61 ±0.08	N.D[a]	1.86 ±0.15	N.D[a]	N.D[a]	N.D[a]	N.D[a]	N.D[a]
	K_m (mM)	0.07 ±0.05	0.12 ±0.06	1.12 ±0.3	N.D[a]	1.49 ±0.25	N.D[a]	N.D[a]	N.D[a]	N.D[a]	N.D[a]
	k_{cat}/K_m (mM^{-1} s^{-1})	50.3	21	0.54	0.005[b]	1.30	N.D[a]	N.D[a]	N.D[a]	N.D[a]	N.D[a]
T207A	k_{cat} (s^{-1})	2.80 ±0.19	2.53 ±0.06	2.42 ±0.06	1.72 ±0.08	3.38 ±0.23	N.D[a]	0.85 ±0.04	N.D[a]	N.D[a]	1.99 ±0.14
	K_m (mM)	0.17 ±0.04	0.19 ±0.02	0.09 ±0.01	2.00 ±0.33	0.30 ±0.09	N.D[a]	0.24 ±0.04	N.D[a]	N.D[a]	0.36 ±0.14
	k_{cat}/K_m (mM^{-1} s^{-1})	16.5	13.3	26.9	0.86	11.3	N.D[a]	3.54	N.D[a]	N.D[a]	5.53
T207G	k_{cat} (s^{-1})	2.11 ±0.23	4.16 ±0.60	4.49 ±0.50	1.10 ±0.14	2.47 ±0.23	N.D[a]	1.41 ±0.23	0.62 ±0.12	N.D[a]	1.89 ±0.14
	K_m (mM)	0.63 ±0.23	0.25 ±0.11	0.21 ±0.06	2.19 ±0.67	0.05 ±0.02	N.D[a]	0.93 ±0.52	1.72 ±0.64	N.D[a]	0.09 ±0.02
	k_{cat}/K_m (mM^{-1} s^{-1})	3.34	16.6	21.4	0.50	49.5	0.03[b]	1.52	0.36	N.D[a]	21.1
T207S	k_{cat} (s^{-1})	2.22 ±0.10	2.13 ±0.2	6.11 ±0.62	1.45 ±0.12	5.30 ±0.82	N.D[a]	0.68 ±0.08	N.D[a]	N.D[a]	1.28 ±0.08
	K_m (mM)	0.05 ±0.01	0.06 ±0.02	0.14 ±0.04	3.57 ±0.72	0.13 ±0.07	N.D[a]	0.49 ±0.21	N.D[a]	N.D[a]	0.58 ±0.11
	k_{cat}/K_m (mM^{-1} s^{-1})	44.4	35.5	43.6	0.41	40.80	N.D[a]	1.39	N.D[a]	0.004[b]	2.21
M306I	k_{cat} (s^{-1})	1.60 ±0.19	2.05 ±0.3	4.91 ±0.52	N.D[a]	3.42 ±0.69	N.D[a]	N.D[a]	N.D[a]	N.D[a]	N.D[a]
	K_m (mM)	0.12 ±0.05	0.44 ±0.13	0.17 ±0.05	N.D[a]	0.55 ±0.28	N.D[a]	N.D[a]	N.D[a]	N.D[a]	N.D[a]
	k_{cat}/K_m (mM^{-1} s^{-1})	13.4	4.7	29	0.01[b]	6.20	N.D[a]	N.D[a]	N.D[a]	N.D[a]	0.08[b]
M306V	k_{cat} (s^{-1})	1.38 ±0.14	0.60 ±0.09	0.92 ±0.15	N.D[a]	0.47 ±0.03	N.D[a]	N.D[a]	N.D[a]	N.D[a]	N.D[a]
	K_m (mM)	0.31 ±0.11	0.66 ±0.35	0.22 ±0.13	N.D[a]	0.63 ±0.13	N.D[a]	N.D[a]	N.D[a]	N.D[a]	N.D[a]
	k_{cat}/K_m (mM^{-1} s^{-1})	4.45	0.91	4.2	N.D[a]	0.75	N.D[a]	N.D[a]	N.D[a]	N.D[a]	0.06[b]
T207A/ M306I	k_{cat} (s^{-1})	1.89 ±0.15	3.15 ±0.46	2.65 ±0.14	N.D[a]	1.60 ±0.14	N.D[a]	1.20 ±0.19	N.D[a]	0.31 ±0.02	1.55 ±0.12
	K_m (mM)	0.53 ±0.14	0.61 ±0.26	0.10 ±0.02	N.D[a]	0.40 ±0.11	N.D[a]	0.49 ±0.23	N.D[a]	2.28 ±0.49	0.07 ±0.02
	k_{cat}/K_m (mM^{-1} s^{-1})	3.6	5.16	26.5	0.10[b]	4	0.02[b]	2.47	N.D[a]	0.14	22.1
T207A/ M306V	k_{cat} (s^{-1})	1.16 ±0.04	2.86 ±0.14	3.44 ±0.31	1.14 ±0.10	0.29 ±0.02	0.56 ±0.04	1.12 ±0.15	N.D[a]	0.18 ±0.01	2.78 ±0.33
	K_m (mM)	0.67 ±0.10	0.52 ±0.10	0.24 ±0.08	0.56 ±0.14	0.12 ±0.03	2.90 ±0.57	0.48 ±0.23	N.D[a]	2.05 ±0.34	0.41 ±0.22
	k_{cat}/K_m (mM^{-1} s^{-1})	1.73	5.5	14.3	2.04	2.4	0.19	2.34	N.D[a]	0.09	6.8

T207G/ M306I	k_{cat} (s^{-1})	N.D[a]	0.62 ±0.12	5.39 ±0.29	0.64 ±0.02	4.33 ±0.12	2.01 ±0.25	1.22 ±0.10	0.51 ±0.06	N.D[a]	2.69 ±0.10
	K_m (mM)	N.D[a]	0.80 ±0.38	0.10 ±0.02	0.74 ±0.09	0.09 ±0.01	0.23 ±0.09	0.45 ±0.16	0.82 ±0.32	N.D[a]	0.11 ±0.02
	k_{cat}/K_m (mM^{-1} s^{-1})	N.D[a]	0.78	53.9	0.86	48	8.7	2.71	0.62	0.004[b]	24.5
T207G/ M306V	k_{cat} (s^{-1})	N.D[a]	0.17 ±0.02	6.17 ±0.37	N.D[a]	4.27 ±0.39	1.68 ±0.17	0.56 ±0.04	0.42 ±0.06	N.D[a]	1.74 ±0.21
	K_m (mM)	N.D[a]	0.54 ±0.15	0.20 ±0.05	N.D[a]	0.27 ±0.07	0.35 ±0.10	0.38 ±0.09	1.35 ±0.54	N.D[a]	0.03 ±0.02
	k_{cat}/K_m (mM^{-1} s^{-1})	N.D[a]	0.31	30.9	0.02[b]	15.8	4.8	1.48	0.32	N.D[a]	58
T207S/ M306I	k_{cat} (s^{-1})	1.26 ±0.19	9.24 ±2.32	8.74 ±1.02	1.45 ±0.10	6.44 ±0.68	N.D[a]	0.76 ±0.06	N.D[a]	0.31 ±0.01	4.54 ±0.77
	K_m (mM)	0.45 ±0.26	0.85 ±0.40	0.04 ±0.02	0.55 ±0.18	0.07 ±0.03	N.D[a]	0.47 ±0.12	N.D[a]	3.85 ±0.37	0.20 ±0.09
	k_{cat}/K_m (mM^{-1} s^{-1})	2.8	10.9	218.5	2.64	92	0.02[b]	1.62	N.D[a]	0.08	22.7
T207S/ M306V	k_{cat} (s^{-1})	0.64 ±0.06	1.59 ±0.31	1.80 ±0.01	N.D[a]	0.62 ±0.08	N.D[a]	0.52 ±0.04	N.D[a]	N.D[a]	1.25 ±0.19
	K_m (mM)	0.39 ±0.20	1.65 ±0.98	0.08 ±0.002	N.D[a]	0.30 ±0.11	N.D[a]	0.92 ±0.26	N.D[a]	N.D[a]	1.02 ±0.43
	k_{cat}/K_m (mM^{-1} s^{-1})	1.64	0.96	22.5	0.02[b]	2.1	N.D[a]	0.57	N.D[a]	N.D[a]	1.23

Steady state kinetic parameters were determined as described in the **Experimental Section**, using a fixed concentration of CoA and ATP, and varied concentration of malonate analog.

[a] Non-detectable. Estimated minimum detection limit is a k_{cat}/K_m of 0.004 mM^{-1} s^{-1}.

[b] Saturation was not achieved and k_{cat}/K_m was calculated by linear regression analysis of the velocity versus substrate concentration plot (See **Figure S 1**)

Table S2. HPLC/ESI-MS analysis of acyl-CoA's produced by MatB catalyzed ligations**.**
[a] See **Figure 2b** for structures of acyl-CoAs.

malonate/ acyl-CoA[a]	Product retention time (mins)[b]	Conversion rate (%)[c]		m/z (Da)[d]	m/z (Da)[e]
		WT	T207G/ M306I		
16/**1**	14.36	91±6	24±1	852.11[g] 403.55[h]	852.11[g] 403.57[h]
17/**2**	16.80	85±8	45±5	866.12[g] 410.56[h]	866.09[g] 410.55[h]
18/**3**	19.25	42±2	91±3	880.13[g] 417.57[i]	880.10[g] 417.55[i]
19/**27**	17.72	60.5±11	91±5	890.12[g] 422.55[h]	890.12[g] 422.56[h]
20/**28**	20.52	81±5	89±2	892.13[g] 423.57[h]	892.10[g] 423.55[h]
21/**29**	21.67	N.D[f]	86±4	894.15[g] 446.57[i]	894.15[g] 446.57[i]
22/**30**	25.73	N.D[f]	92±6	908.17[g] 431.58[h]	908.17[g] 431.59[h]
23/**31**	24.99	N.D[f]	62±7	928.13[g] 884.14[j]	928.11[g] 884.14[j]
24/**32**	12.41	19±0.5	N.D[f]	868.10[g] 411.54[h]	868.10[g] 411.58[h]
25/**33**	14.40	1.54±0.02	14±2	882.12[g] 418.55[h]	882.12[g] 418.56[h]
26/**34**	19.61	N.D[f]	86±3	921.14[g] 460.06[i]	921.14[g] 460.06[i]

[b] See **Experimental Section** for HPLC conditions.
[c] Percent conversions were determined by HPLC and calculated by dividing the integrated area of the acyl-CoA product by the sum of the integrated area of the product plus the integrated area of the remaining CoA. See **Experimental Section** for reaction conditions.
[d] Calculated mass of acyl-CoA product
[e] Observed mass of acyl-CoA product
[f] Non-detected. Estimated minimal detection limit is 0.2 % conversion.
[g] $[M-H]^{-1}$
[h] $([M-CO_2-2H]^{-2})/2$
[i] $[M-2H]^{-2}/2$
[j] $[M-CO_2-H]^{-1}$

Table S3. FT-ICR mass spectrometry analysis of *trans*-AT catalyzed reactions.

Enzyme/ acyl-CoA[a]	Acylated product[b]	Calculated mass (Da)[c]	Observed mass (Da)[d]	Mass error (ppm)[e]	Percent conversion (%)[f]	Detected in negative control[g]	Activity ratio[h]
DSZS/**1**	Malonyl-ACP6$_{DEBS}$	11707.73	11707.68	-4.27	84	N	-
DSZS/**2**	Methyl-ACP6$_{DEBS}$	11722.76	N.D[i]	-	-	-	-
DSZS/**3**	Ethyl-ACP6$_{DEBS}$	11736.77	11736.63	-11.9	1	Y	1.0
DSZS/**27**	Propargyl-ACP6$_{DEBS}$	11746.76	N.D[i]	-	-	-	-
DSZS/**28**	Allyl-ACP6$_{DEBS}$	11748.77	N.D[i]	-	-	-	-
DSZS/**29**	Isopropyl-ACP6$_{DEBS}$	11750.79	N.D[i]	-	-	-	-
DSZS/**30**	Butyl-ACP6$_{DEBS}$	11764.80	N.D[i]	-	-	-	-
DSZS/**31**	Phenyl-ACP6$_{DEBS}$	11740.78	11740.72	-5.11	2	Y	1.2
DSZS/**32**	Hydroxy-ACP6$_{DEBS}$	11724.73	N.D[i]	-	-	-	-
DSZS/**33**	Methoxy-ACP6$_{DEBS}$	11738.75	N.D[i]	-	-	-	-
DSZS/**34**	Azidoethyl-ACP6$_{DEBS}$	11777.77	N.D[i]	-	-	-	-
MCAT/**1**	Malonyl-ACP6$_{DEBS}$	11707.73	11707.68	-4.27	85	N	-
MCAT/**2**	Methyl-ACP6$_{DEBS}$	11722.76	N.D[i]	-	-	-	-
MCAT/**3**	Ethyl-ACP6$_{DEBS}$	11736.77	N.D[i]	-	-	-	-
MCAT/**27**	Propargyl-ACP6$_{DEBS}$	11746.76	N.D[i]	-	-	-	-
MCAT/**28**	Allyl-ACP6$_{DEBS}$	11748.77	N.D[i]	-	-	-	-
MCAT/**29**	Isopropyl-ACP6$_{DEBS}$	11750.79	N.D[i]	-	-	-	-
MCAT/**30**	Butyl-ACP6$_{DEBS}$	11764.80	N.D[i]	-	-	-	-
MCAT/**31**	Phenyl-ACP6$_{DEBS}$	11740.78	11740.70	-6.81	1	Y	1.7
MCAT/**32**	Hydroxy-ACP6$_{DEBS}$	11724.73	N.D[i]	-	-	-	-
MCAT/**33**	Methoxy-ACP6$_{DEBS}$	11738.75	N.D[i]	-	-	-	-
MCAT/**34**	Azidoethyl-ACP6$_{DEBS}$	11777.77	N.D[i]	-	-	-	-
KirCII/**1**	Malonyl-ACP5$_{Kir}$	16664.43	N.D[i]	-	-	-	-
KirCII/**2**	Methyl-ACP5$_{Kir}$	16678.45	N.D[i]	-	-	-	-
KirCII/**3**	Ethyl-ACP5$_{Kir}$	16692.46	16692.51	3.00	15	N	-

KirCII/**27**	Propargyl-ACP5$_{Kir}$	16702.45	16702.48	1.80	8	N	-
KirCII/**28**	Allyl-ACP5$_{Kir}$	16704.46	16704.49	1.80	15	N	-
KirCII/**29**	Isopropyl-ACP5$_{Kir}$	16706.48	N.D[i]	-	-	-	-
KirCII/**30**	Butyl-ACP5$_{Kir}$	16720.49	N.D[i]	-	-	-	-
KirCII/**31**	Phenyl-ACP5$_{Kir}$	16696.47	16696.45	-1.20	2	Y	0.7
KirCII/**32**	Hydroxy-ACP5$_{Kir}$	16680.42	N.D[i]	-	-	-	-
KirCII/**33**	Methoxy-ACP5$_{Kir}$	16694.44	N.D[i]	-	-	-	-
KirCII/**34**	Azidoethyl-ACP5$_{Kir}$	16733.46	16733.45	-0.60	2	N	-

[a] See **Figure 2** for structures of acyl-CoAs.

[b] ACP6$_{DEBS}$ refers to ACP6 of module 6 from the erythronolide B PKS, ACP5$_{Kir}$ refers to ACP5 of module 5 from the kirromycin PKS.

[c] Calculated monoisotopic mass. See **Experimental Section** for details.

[d] Observed mass of acylated ACP product.

[e] Mass error = (Mass$_{obs}$-Mass$_{calcd}$/Mass$_{calcd}$) x 10^6

[f] Percent conversion = (Area$_{acyl\text{-}ACP}$/Area$_{\textit{holo}\text{-}ACP}$+Area$_{acyl\text{-}ACP}$)

[g] Reactions were performed in the absence of *trans*-AT enzyme to identify background acylation.

[h] Activity ratio = conversion with enzyme/conversion without enzyme. Acyl-CoA is considered a substrate only when the acylation in the absence of *trans*-AT is zero.

[i] Non detected.

Table S4. Oligonucleotide sequences used in this study. Altered codons are underlined.

Primer name	Primer sequence
MatB-T207G-FOR	GCCCTGCCGATCTTTCATGGGCACGGTCTGTTCGTTG
MatB-T207G-REV	CAACGAACAGACCGTGCCCATGAAAGATCGGCAGGGC
MatB-T207A-FOR	GCCCTGCCGATCTTTCATGCGCACGGTCTGTTCGTTG
MatB-T207A-REV	CAACGAACAGACCGTGCGCATGAAAGATCGGCAGGGC
MatB-T207S-FOR	GCCCTGCCGATCTTTCATTCTCACGGTCTGTTCGTTG
MatB-T207S-REV	CAACGAACAGACCGTGAGAATGAAAGATCGGCAGGGC

Supplementary Methods

Synthesis of 2-methoxymalonate (25). Dimethyl methoxymalonate (0.85 mL, 6.2 mmol) and NaOH (2.4g, 60 mmol) were added to a round bottom flask containing 10 mL H_2O and the mixture was stirred for 6 hours at 65°C. The solution was cooled on ice and 10 mL ice cold 12.1N HCl was added. The solution was extracted 6x with diethyl ether. The combined organic extracts were dried over $MgSO_4$ and filtered. The solvent was removed under vacuum to give 2-methoxymalonate as a white solid (0.323 g, 39%). ^{1}H-NMR (300 MHz, D_2O): 4.44 (s, 1H), 3.30 (s, 3H) (See **Figure S4**).

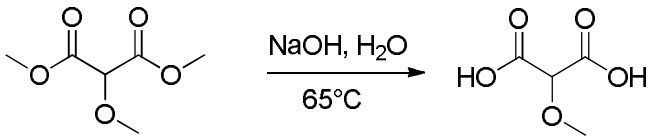

25

Synthesis of 2-(2-azidoethyl)malonic acid (26). Diethyl cyclopropyl-1,1-dicarboxylate (50 mmol), sodium azide (100 mmol) and triethylamine hydrochloride (100 mmol) were dissolved in 50 mL NMP. The reaction was stirred at reflux for 60 hours at 90°C. The reaction was cooled and diluted with 200 mL diethyl ether. The organic layer was washed 7x with 100 mL H_2O, washed with brine, dried over $MgSO_4$, and filtered. The solvent was removed under vacuum to yield diethyl 2-(2-azidoethyl)malonate (**26a**) as a brown oil (8.9 g, 78% yield). ^{1}H-NMR (300 MHz, $CDCl_3$): δ 4.2 (q, *J* = 7.2 Hz, 4H), 3.47 (t, *J* = 7.5 Hz, 1H), 3.38 (t, *J* = 6.6 Hz, 2H), 2.1 (q, *J* = 7.5 Hz, 2H), 1.25 (t, *J* = 7.2 Hz, 6H) (See **Figure S5**).

26a (2.5 mmol) was added to 15% w/v aqueous NaOH (7.5 mmol) and the mixture was stirred for 48 hours at room temperature. 10 mL H_2O was added, and the aqueous solution was washed with diethyl ether. The solution was cooled on ice and HCl was slowly added to adjust the pH to 2. The solution was extracted 6x with diethyl ether. The combined organic extracts were washed with brine, dried over $MgSO_4$, and filtered. The solvent was removed under vacuum to give 2-(2-azidoethyl)malonic acid (**26)** as a white solid (0.225 g, 52%). ^{1}H-NMR (300 MHz, D_2O): 3.4 (t, *J* = 7.2 Hz, 1H), 3.27 (t, *J* = 6.6 Hz, 2H), 2.0 (q, *J* = 6.9 Hz, 2H).

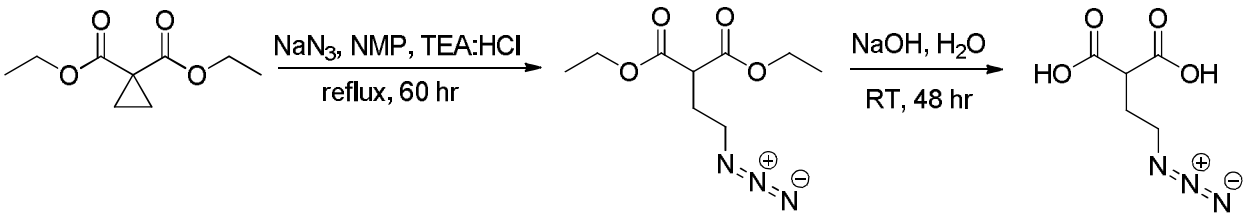

26a **26**

Synthesis of 2-(prop-2-yn-1-yl)malonic acid (19). Dimethyl propargylmalonate (0.94 mL, 6.2 mmol) and NaOH (2.4g, 60 mmol) were added to a round bottom flask containing 10 mL H_2O and the mixture was stirred for 6 hours at 65°C. The solution was cooled on ice and 10 mL ice cold 12.1N HCl was added. The solution was extracted 6x with diethyl ether. The combined organic extracts were dried over $MgSO_4$ and filtered. The solvent was removed under vacuum to give 2-(prop-2-yn-1-yl)malonic acid as a white solid (0.298 g, 34%). ^{1}H-NMR (300 MHz, D_2O): 3.59 (t, J = 7.2 Hz, 1H), 2.6 (d of d, J = 7.2 Hz, J = 2.7 Hz, 3H), 2.26 (t, J = 2.7 Hz, 1H) (See **Figure S6**).

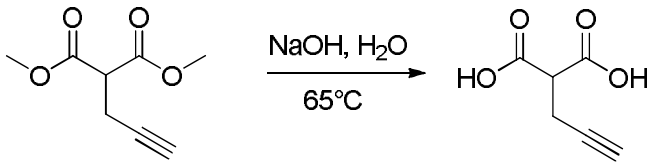

19

Cloning DSZS and MCAT. The gene for DSZS[2] from *Sorangium cellulosum* was synthesized by GeneScript and subcloned into pET28a *via Nco*I and *Hin*dIII restriction sites. The *FabD* gene coding MCAT was PCR amplified from genomic DNA of *Streptomyces coelicolor* A3(2) using the following primers: 5'–CGGATCCATATGCTCGTACTCGTCGCTC–3' and 5'–CGGCTCGAGTCAGGCCTGGGTGTGCTCG–3' (restriction sites underlined). *FabD* was cloned into pET28a via *Nde*I and *Xho*I restriction sites.

Site-directed mutagenesis. Site-specific MatB variants were constructed by using the Stratagene QuikChange II Site-Directed Mutagenesis Kit, as described by the manufacturer. Constructs were confirmed to carry the correct mutation(s) by DNA sequencing. Oligonucleotide sequences used for mutagenesis are given in **Table S4**.

Expression and purification of WT and mutant MatB. *E. coli* BL21(DE3) pLysS competent cells were transformed with the suitable plasmid and positive transformants were selected on LB agar supplemented with 30 μg/mL kanamycin. A single colony was transferred to LB (3 mL) supplemented with kanamycin (30 μg/mL) and grown at 37 °C and 250 rpm overnight. The culture was used to inoculate LB media (1L) supplemented with kanamycin (30 μg/mL). One liter culture was incubated at 37 °C and 250 rpm to an $O.D_{600}$ of 0.6, at which time protein synthesis was induced by the addition of IPTG to a final concentration of 1 mM. After incubation at 18 °C and 200 rpm for 18 h, cells were collected by centrifugation at 5,000 *g* for 20 min, and resuspended in 100 mM Tris-HCl pH 8.0 (20 mL) containing

NaCl (300 mM) and then lysed by sonication. Following centrifugation at 10,000 *g*, the soluble extract was loaded onto a 1 mL HisTrap HP column (GE Healthcare, Piscataway, NJ) and purified by fast protein liquid chromatography using the following buffers: wash buffer [20 mM phosphate (pH 7.4) containing 0.5 M NaCI and 20 mM imidazole] and elution buffer [20 mM phosphate (pH 7.4) containing 0.5 M NaCI and 200 mM imidazole]. The purified protein was concentrated using an Amicon Ultra 10,000 MWCO centrifugal filter (Millipore Corp., Billerica, MA) and stored as 10% glycerol stocks at -80 ℃. Protein purity was verified by SDS-PAGE. Protein quantification was carried out using the Bradford Protein Assay Kit from Bio-Rad.

Determination of MatB kinetic parameters

Enzyme assays were carried out in a total volume of 200 μl 100 mM sodium phosphate (pH 7) containing 2 mM $MgCl_2$ and 1 μg pure enzyme. Kinetic parameters k_{cat} and K_M were determined with **16-23, 25-26** as variable substrates, keeping ATP and coenzyme A concentrations constant (0.4 mM and 0.2 mM, respectively). Each experiment was performed in triplicate. The incubation time of assays was 5-40 min, depending on the enzyme/substrate, such that product formation was still linear with respect to time. Aliquots were removed and quenched with an equal volume of ice-cold methanol, centrifuged at 10,000 *g* for 10 min, and cleared supernatants used for HPLC analysis on a Varian ProStar HPLC system. A series of linear gradients was developed from 0.1% TFA (A) in water to methanol (HPLC grade, B) using the following protocol: 0-32 min, 80% B; 32-35 min, 100% A. The flow rate was 1 mL/min, and the absorbance was monitored at 254 nm using Pursuit XRs C18 column (250 x 4.6 mm, Varian Inc.). Concentration of product formed was determined as described above, and initial velocities were fitted to the Michaelis-Menten equation using SigmaPlot.

Expression and purification of DSZS, MCAT, DEBS *holo*-ACP6, KirCII, and Kir *holo*-ACP5.

DSZS was over-expressed in *E. coli* BL21(DE3) as a C-terminally His_6-tagged fusion protein and purified as previously described[2]. MCAT was over-expressed in *E. coli* BL21(DE3) as an N-terminally His_6-tagged fusion protein and purified as previously described[3]. *Apo*-ACP6 from the *Saccharopolyspora erythraea* erythromycin biosynthetic gene cluster was cloned in pET28a as described[4] and over-expressed as the *apo*-ACP in *E. coli* BL21(DE3) as an N-terminally His_6-tagged fusion protein as previously described[3]. The kirromycin *trans*-AT KirCII, harbored in pET52 3C/LIC[5], was over-expressed in Rosetta2(DE3) pLysS as an N-terminally His_6-tagged fusion protein as previously described[5]. DEBS *holo*-ACP6 and Kir *holo*-ACP5 were prepared via *in vivo* phosphopantetheinylation by co-expression of *apo*-$ACP6_{DEBS}$ or *apo*-$ACP5_{Kir}$ with Sfp. This was achieved using a two-plasmid system: ACP5-pET52 3C/LIC (ampicillin resistant) or ACP6-pET28a (kanamycin resistant) with Sfp-pSU20 (chloramphenicol

resistant)[6]. Each ACP/Sfp pair was over-expressed in *E. coli* BL21 (DE3) pLysS grown at 37 °C with shaking at 250 rpm. DEBS *holo*-ACP6 was purified as described for MatB. KirCII and Kir *holo*-ACP5 were purified as previously described[5].

Supplementary References

1. Piasecki, S.K. *et al.* Employing modular polyketide synthase ketoreductases as biocatalysts in the preparative chemoenzymatic syntheses of diketide chiral building blocks. *Chem. Biol.* **18**, 1331-1340 (2011).
2. Wong, F.T., Jin, X., Mathews, II, Cane, D.E. & Khosla, C. Structure and Mechanism of the trans-Acting Acyltransferase from the Disorazole Synthase. *Biochemistry* **50**, 6539-6548 (2011).
3. Koppisch, A.T. & Khosla, C. Structure-based mutagenesis of the Malonyl-CoA: Acyl carrier protein transacylase from Streptomyces coelicolor. *Biochemistry* **42**, 11057-11064 (2003).
4. Ye, Z., Bair, M., Desai, H. & Williams, G.J. A photocrosslinking assay for reporting protein interactions in polyketide and fatty acid synthases. *Molecular BioSystems* **7**, 3152-3156 (2011).
5. Musiol, E.M. *et al.* Supramolecular templating in kirromycin biosynthesis: the acyltransferase KirCII loads ethylmalonyl-CoA extender onto a specific ACP of the trans-AT PKS. *Chem. Biol.* **18**, 438-444 (2011).
6. Bartolome, B., Jubete, Y., Martinez, E. & Delacruz, F. Construction And Properties Of A Family Of Pacyc184-Derived Cloning Vectors Compatible With Pbr322 And Its Derivatives. *Gene* **102**, 75-78 (1991).